Hindawi
Advances in Civil Engineering
Volume 2023, Article ID 6858371, 11 pages
https://doi.org/10.1155/2023/6858371

Research Article

An Investigation on Soil Amplification through Site Factors Used in Seismic Design Codes

Hayri Baytan Ozmen

Department of Civil Engineering, Usak University, 64200 Usak, Turkey

Correspondence should be addressed to Hayri Baytan Ozmen; baytan.ozmen@usak.edu.tr

Received 1 July 2022; Revised 23 January 2023; Accepted 3 February 2023; Published 17 February 2023

Academic Editor: Bruno Dal Lago

This article aims to investigate the site amplification through site coefficients given in the seismic codes. A set of 84 ground motion records in a base rock form and targeted to have different frequency contents was formed. The surface forms of these records altered by 100 different soil conditions were determined. Using this set of 8400 ground motion records, site amplification phenomenon is examined. After a PGA of 0.3 g, ground motions have similar behaviour in terms of short period amplification. Numerical figures as average and with a safety level of 84% for the S_S and S_1 site coefficients were given and compared with the code which are observed to be unconservative for stiff soils and too conservative for soft soils. Linking S_S with a V_S value of 600 m/s and S_1 with a V_S value of 120 m/s seems to be useful to understand some amplification behaviours. The variability of ZB and ZC site classes for short period site coefficient and ZE and ZD site classes for midperiod site coefficient seems to be greater when compared to others.

1. Introduction

Seismic loadings are the major sources of structural damage in many earthquake prone countries [1]. Local site conditions are the parameters that have the greatest impact on the characterisation of seismic effects on structures per seismic codes. For this reason, the examination of the change of earthquake waves from the bedrock to the ground surface, where most of the engineering structures are found, is among the important topics of earthquake and structural engineering. When passing through the different layers between bedrock and surface, seismic waves may be significantly amplified. Site amplification may be regarded as the ratios of ground motion intensity quantities at a soil site to their counterparts at a rock site [2]. This amplification depends on the local site conditions. Consequently, seismic design codes take into account the local site conditions by defining "Site Classes/Types" which are linked to different seismic loading spectra. In one of the earlier studies, Seed et al. [3] proposed normalized spectral forms that include site-dependent ground motion characteristics based on earthquake records with peak ground accelerations (PGA) greater than 0.05 g. Their work resulted in four distinct spectral shapes for different site conditions.

The seismic codes in most of the earthquake prone countries use a soil classification by taking into account the soil properties of the upper 30 m of the ground [4–7]. Especially, the V_{s30} value is an equivalent velocity value determined as 30 m divided by the travelling time of S waves from 30 m to surface. Many codes include similarities with the NEHRP recommended approaches. The determination of NEHRP site factors is mainly based on the study by Borcherdt [8] that used the strong-motion recordings of the 1989 Loma Prieta, California earthquake. The NEHRP provisions describe the site factors as ratios of reference site (with $V_{s30} = 760$ m/s) pseudospectral accelerations at $T = 0.2$ s and $T = 1.0$ s. The V_{s30} value of 760 m/s is the boundary of B and C site classes. The required site class spectrum was established by using the ratios of the pseudospectral accelerations at $T = 0.2$ s and $T = 1.0$ s of that class to the reference site. These ratios are called "site coefficients" and they reflect the soil amplification. Recent Turkish seismic code also followed the same methodology [6]. Site coefficients tend to increase with decreasing soil stiffness, i.e., V_{s30} value.

Dobry et al. examined and explained the site amplification factors and a procedure for site classification of code provisions for buildings and other structures (1994 and 1997 NEHRP Provisions, 1997 UBC) [9]. Huang et al. [10] investigated the suitability of NEHRP site coefficients using ground motion prediction equations developed under NGA-West1 project [11]. They determined site coefficients for V_{s30} values between 150 m/s and 1500 m/s by normalizing the estimated spectral values with respect to reference site of $V_{s30} = 760$ m/s. They concluded that average NGA site amplification factors show a clear dependency on period for V_{s30} smaller than 270 m/s and for some cases are considerably greater than the NEHRP site coefficients, especially for longer periods. Borcherdt [12] also examined the site coefficients considering $V_{s30} = 1050$ m/s for the reference rock site. He reported that the next generation attenuation coefficients are shown to agree well with adopted site coefficients at low levels of input motion of 0.1 g. For motions with higher intensity, he observed diverging values for site classes *C* and *D* for short and midperiod coefficients, respectively. Sandıkkaya et al. [13] suggested an empirical site amplification model that can be used in ground motion prediction equations derived for shallow crustal regions and determined site coefficients for *C*, *D*, and *E* site classes. Most of the presented values are significantly lower than the NEHRP recommendations [4]. Seyhan and Stewart [14] using their semiempirical nonlinear site model that is developed under NGA-West2 project [15] concluded that for stronger shaking levels and class *C* and *D* soils, the site coefficients are slightly greater and coefficients for soft soil (class *E*) are conservative. Findings of the Seyhan and Stewart [14] study were implemented in the 2015 edition of NEHRP provisions [16] and also employed in the seismic design load definitions by ASCE/SEI 7–16 [17]. Dhakala et al. [18] conducted a numerical parametric study in order to understand the effect of soil characteristics on seismic demand and to examine the rationality of the current site-specific seismic design spectra [7]. They reported that stiff soils generally tend to have a higher spectral acceleration response in comparison to soft soils although it is less prominent for high intensity bed rock motions. Additionally, for medium to hard soils, the spectral acceleration response at short period is significantly underestimated by the provisions.

Lussou et al. compared the site effect section of building codes (ECU and UBC97) with the set of data provided by the Kyoshin network [19]. They reported that concerning spectral shapes and site coefficients, analyses results are found to be in good agreement with ECS and UBC97 only if category *B* is taken as reference. Işık et al. [20] conducted a study to investigate the effect of site-specific design spectrum on earthquake building parameters considering Marmara region of Turkey. They concluded that the seismicity characteristics of the considered geographic location significantly influence the seismic displacements. Another study by Yavaşoğlu et al. also underlines the importance of site features on seismic behaviour [21]. Strukar et al. investigated the seismic damage with respect to site characteristics by spectral matching [22].

Table 1: Site classification [6, 17].

Site class	Soil type	V_{s30} (m/s)
ZA	Hard rock	$V_{s30} > 1500$
ZB	Rock	760–1500
ZC	Very dense soil/soft rock	360–760
ZD	Stiff soil	180–60
ZE	Soft soil	$V_{s30} < 180$
ZF	Soils requiring site-specific evaluation	N/A

When the present literature on the subject is evaluated, various site models and approaches yielding different results for site coefficients may be observed [23]. This study is conducted in order to contribute the discussion on the site coefficients. A collection of 84 ground motion records is formed in base rock characteristics. This set aimed to have various frequency contents to have unbiased evaluations. Surface form of these records for 100 different site conditions was determined using ProShake 2.0 software [24]. Evaluations on the obtained 8400 ground motion records were made. Many studies used ground motions recorded at passed seismic events. Tens or hundreds of records from the same event possibly with similar frequency content may be considered in the studies. This may result in unbalanced results more weighted towards highly used events. The methodology considered in this article may have unique features from the mentioned perspective. Average and with 84% probability of not exceedance site coefficients for site classes ZB to ZF are given and compared with current codes, and the variability of site coefficients in terms of different site classes is discussed. By the features mentioned above, similar studies may be considered to be limited in the literature.

2. Considered Site Conditions

Detailed information on used soil profiles is given in the article by Ozmen et al. [25]. Properties of soil layers consisting the considered sites are also presented in the supplementary spread sheet files of the mentioned study. Determination of site classification is made according to the ASCE/SEI 7–16 [17] and Turkish Building Seismic Code [6]. These documents categorize local site classes considering the top 30 m shear wave velocity at the site as given in Table 1.

A total of 100 different site conditions were considered in scope of the study. The features of soil layers in accounted sites were determined in a parametric approach to investigate code suggested values. Beyaz [26] conducted a study related to the soil profiles at seismological recording stations in Turkey using borehole geophysics. This article was referred in establishment of the features of soil layers. Site classifications and V_{s30} values of the considered sites are given in Figure 1. Since the ZF is a special site type, it may have different V_{s30} values. As illustrated in Figure 1, the considered soil profiles have a range of different V_{s30} values in their defined velocity ranges.

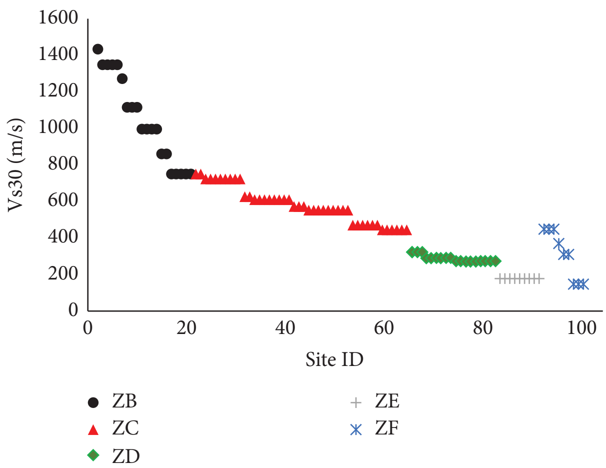

FIGURE 1: Site classifications and V_{s30} values of the considered sites.

3. The Ground Motion Set and Analyses

As mentioned previously, the ground motion set consists of surface form of 8400 records obtained by convolution of 84 ground motions records in base rock form altered by 100 different soil profiles. As the 84 base rock ground motions are the main inputs of the total record set, great importance is given to have a set inconsistence with the nature and including records with various frequency content. Having real earthquake records as many as possible in a ground motion set is ideal to have a set in compliance with nature. Real earthquake records taken from stations on the hard rock in compliance with the assumed bed rock characterisation are intended to be used for input acceleration record set. To have comprehensive evaluations, records having diverse frequency content and intensity values are tried to be selected.

Peak ground acceleration (PGA) was used as the main parameter in selection of input acceleration records since it is taken as the intensity indicator in many seismic codes. The earthquake recordings having PGA values in a range of 0.0 and 0.60 g are picked with 0.05 g increase in each group. Eight records in the initial 4 groups (0–0.20 g), seven in the next 4 groups (0.20–0.40 g), and six earthquake records in the last (0.40–0.60 g) 4 groups were considered. Value of 0.6 g is taken as the final value since ground motions having a PGA of larger than 0.60 g have low occurrence and it is difficult to find such many high intensity records. During their travel from bed rock to the surface, the amplitudes of the records are generally expected to be increased by the soil layers they passed through. Therefore, by using greater amount of records with lower amplitude for the input records, it is intended to get a more evenly distributed output record intensities.

Intensity diversity of the records are provided with selection of records with diverse PGA values. Frequency content diversity in each 0.05 g increase is arranged based on the peak ground velocity (PGV)/peak ground acceleration (PGA) ratio and predominant period and mean period [27] values. As it is known, for a record, the period of the wave with the largest intensity is the predominant period. For a simple harmonic wave, the PGV/PGA value has “period/ 2π” value [28]. PGV/PGA ratio is a significant indicator of the shape of acceleration spectrum and frequency content [29–32]. When current sources of natural earthquake records are examined, significant limitations and inadequacies may be seen in forming a fully natural acceleration record set with the desired features [33, 34].

Having as many as real earthquake records is preferred for an evaluation study. Additionally, these records should have different features to characterise whole behaviour range and get unbiased results [35]. However, high shear wave velocity requirement of recording station representing a bedrock level (around 1500 m/s) and desired diverse frequency content greatly limits the number of available records. If there is not enough number of records for some PGA intervals, alternative methods had to be used; these are deconvolution, scaling, or producing synthetic records. Deconvolution is the process of obtaining base rock form of surface records for known soil profiles.

When performing the scaling process, a major factor is the scale value to be used. The scale value should be a value that does not disturb the properties of the original record. Scaling modifies the amplitude of the ground motion without changing the frequency content. In previous studies, it is reported that higher intensity ground motions tend to be richer in higher period waves [36]. Therefore, scaling records with coefficients too different from unity is likely to bother the intensity and frequency content relation [37]. If some recommendations in present literature are examined, it is concluded that spectral behaviour of the records becomes unclear if the records are scaled outside the 0.25–4.00 range [38, 39]. For linear analyses, a maximum value of 4.0 is suggested, and for nonlinear analyses, a factor between 0.5 and 2.0 is reported to be more suitable [40–42].

A suitable scale range should be decided considering these factors. In order to get accurate results without altering the frequency content-intensity connection of the ground motion records, the minimum and the maximum scale values are selected as 0.70 and 1.30. The considered range is much narrower than observed in present literature. For each PGA step, care is given to obtain acceleration records with diverse features in terms of earthquake features, frequency content, fault type, and source type (natural, deconvolutional, scaled, and synthetic).

The relationships between intensity (PGV) and frequency content indicators (PGV/PGA ratio, mean period (T_M) [27]) for the base records used in the study is shown in Figure 2. No cases of separation or being in the extremities at the graphs by the earthquakes other than natural records are seen in the figure. This may be considered as a sign that the used records are in accordance with the properties of natural records. It is noteworthy that the records other than the natural ones are mostly needed to be employed for greater intensity ground motions since there are no recorded motions with desired feature. This makes them more noticeable in the figure when compared with natural ones.

PGV is reported to be the parameter with maximum correlation with other ground motion indicators in literatures [43, 44] and it has significant association with the seismic damage of different kinds of structures [45–47].

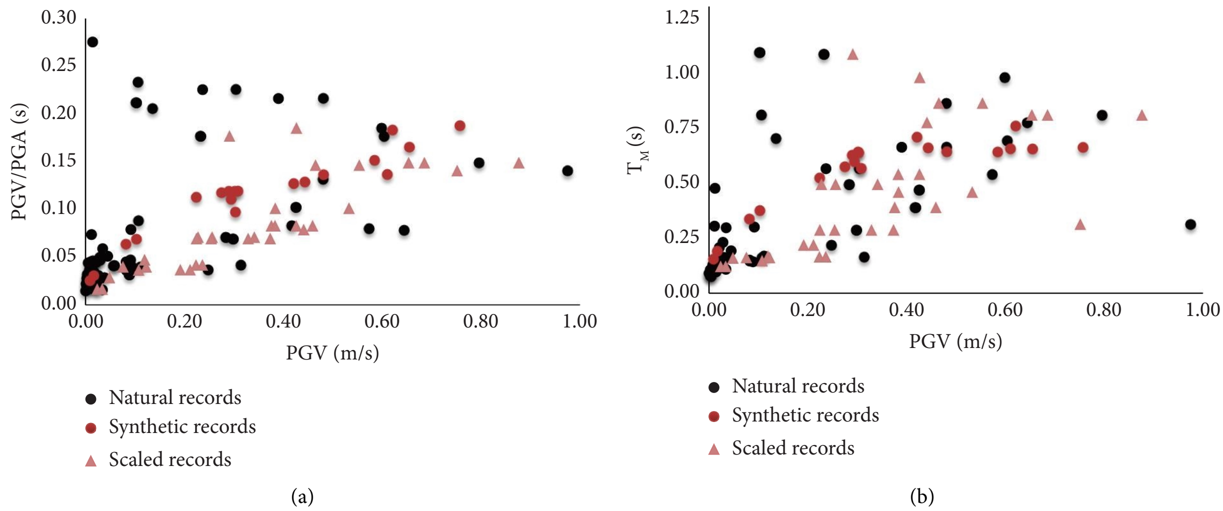

Figure 2: The relationships between frequency content and intensity factors for the considered records. (a) PGV and PGV/PGA relationship. (b) PGV and T_M relationship.

Therefore, it is used as an intensity parameter to examine the frequency content and intensity relation of used ground motion records in Figure 2.

The base 84 records which are aimed to be consistent with base rock characterisation with various intensity and frequency content are used as input records. The output forms of these records at the surface of the 100 soil profiles are determined by ProShake 2.0 software [24]. A collection of 8400 ground motion records with diverse site classes, intensity, and frequency content are obtained. The establishment of the base input acceleration records are explained in more detail in the study by Ozmen et al. [25]. The properties and all used output 8400 records are provided in the attached files to the mentioned article, as well.

4. Analyses Results

As mentioned previously, many seismic codes define the acceleration spectra using the site coefficients which are ratios of pseudospectral accelerations at $T = 0.2$ s and $T = 1.0$ s to reference site of $V_{s30} = 760$ m/s. Therefore, behaviour of spectral accelerations at $T = 0.2$ s (S_S) and $T = 1.0$ s (S_1) are primarily investigated.

4.1. The Relation of Input and Output S Values. Figure 3 illustrates the relationships between input and output S_S and S_1 values. In Figures 3(a) and 3(c), the $x = y$ line, which is the border between amplification and deamplification, is also given. Amplification is the case in which the S value in the surface of the site is bigger than the one at the bedrock level. Deamplification is the case in which the S value is decreased by the soil layers that the ground motion passed through. Note that, in Figures 3(b) and 3(d), the number of amplified cases over the number of total cases is given. The y axis does not show how much the ground motion intensity is amplified, but how frequent is the amplification phenomenon. As can be seen from the figures, the amplified cases are more common as the values are generally greater than 0.5 especially for the low-intensity region. However, amplification ratio seems to decrease with increasing intensity even if there are greatly amplified cases for all intensity levels. In order to observe this phenomenon more closely, distribution of the ratio of amplified cases to the total cases are examined for intensity intervals of 0.1 g (Figure 3(b)).

According to Figure 3(b), for small values, amplifications are almost certain. Up to 0.1 g range, amplification ratio reaches 97%. It gradually decreases to around 75% for 0.5 g. After 0.5 g, there is a significant fall to 40% ratio, and it ranges around 30–44% band. 0.5 g seems to be a corner value for S_S.

Amplification is more pronounced for S_1 than the S_S value per Figures 3(c) and 3(d). Data are located mostly in the upper section of the $x = y$ line. The ratio of amplification starts with almost 100% and gradually decreases to 90% for 0.6-0.7 g S_1 range. No sharp change is observed for S_1.

4.2. The Relation of S_S and S_1 Amplification with V_{s30}. Relation of S_S and S_1 amplification with V_{s30} may be of interest as it is the basis of many seismic codes. Figure 4 shows the V_{s30} and amplification ratio (surface value/bedrock value) of S_S and S_1 for different PGA ranges. As amplification at the surface level is not only dependent on the stiffness of the underlying soil but also on the intensity of the bedrock ground motions, they are grouped as per the PGA at bedrock level [18, 48].

Figures 4(a) and 4(c) looks very chaotic with seemingly arbitrarily distributed points due to high scatter. In such cases, trend lines may be useful tools to identify what the majority of data points indicate. Exponential trend lines are given in Figures 4(b) and 4(d) to make the information in the preceding figures more evident. When Figure 4(b) is examined, up to a PGA of 0.2 g S_S is less amplified with increasing soil stiffness indicated by V_{s30}. Ground motions between 0.2 and 0.3 g has an increasing amplification with flatter increment. In this sense, 0.2 g is observed to be an edge value for PGA. After a PGA of 0.3 g, all ground motions

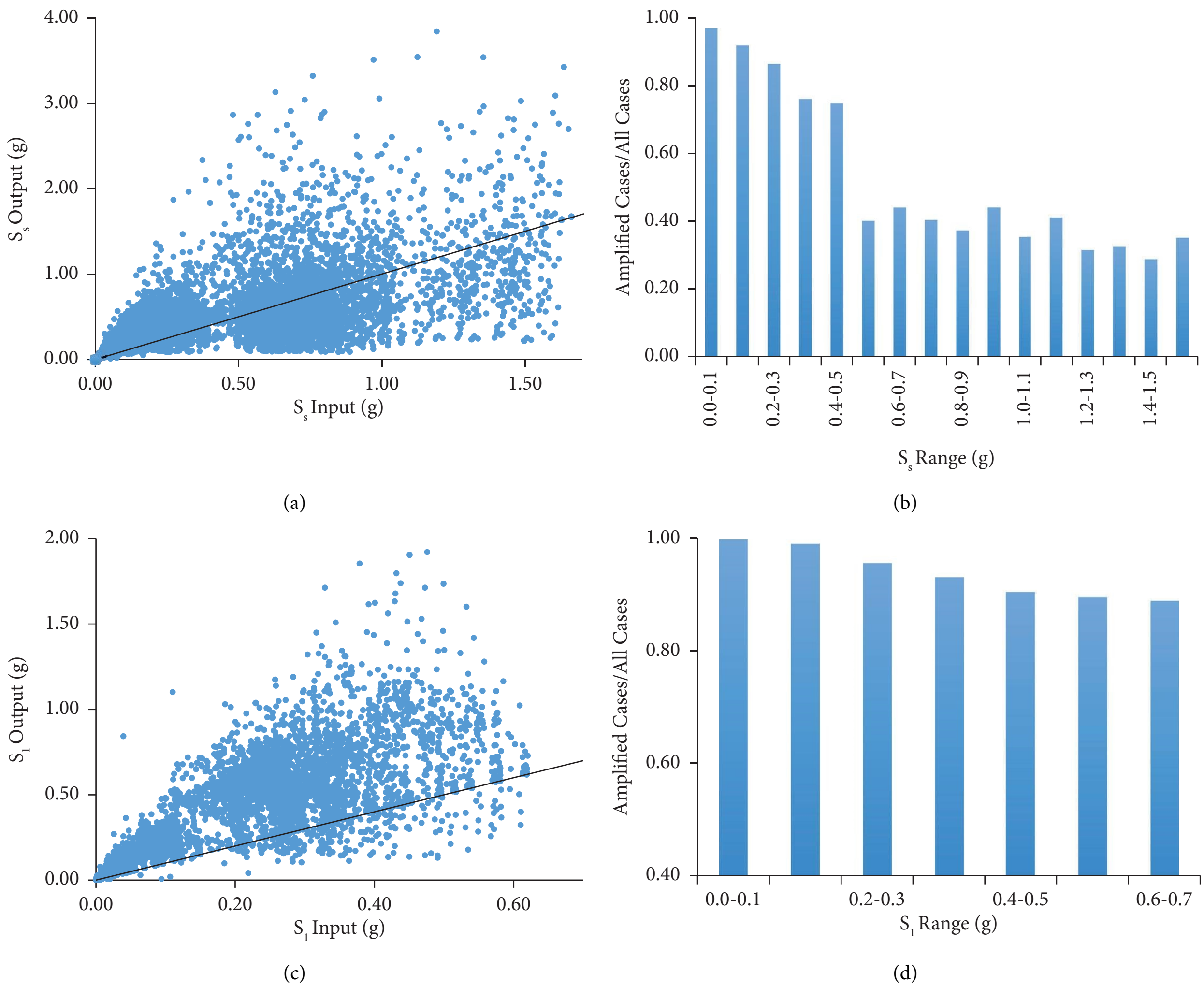

Figure 3: The relationships between input and output S_S and S_1 values. (a) Input and output relation for S_S. (b) Ratio of amplified cases for different S_S ranges. (c) Input and output relation for S_1. (d) Ratio of amplified cases for different S_1 ranges.

have the same behaviour of increasing amplification with increasing soil stiffness with fully coinciding trend lines. 0.3 g PGA seems to be a starting point for ground motions to have a more common behaviour.

For soft soils (i.e., low values of V_{s30}), the amplification (especially S_s) decreases for increasing level of input PGA. This is attributable to soil nonlinearity: for higher input PGA, damping ratio of soils increases accordingly with shear strains in soil. The increase in damping ratio causes the reduction of amplification for high values of input PGA at rock. The effect of damping ratio is particularly pronounced for higher frequencies, and this is the reason for the reduction of amplification being more evident for S_s (high frequency) than in S_1 (low frequency) coefficient. This is more emphasized for the analyses with intensities higher than 0.2, especially 0.3 g PGA.

Even if Figure 4(c) looks chaotic, trend lines on Figure 4(d) have a more collective behaviour of decreasing amplification ratio with increasing soil stiffness. Only differences are the grade of change. S_1 amplification of ground motions with a PGA greater than 0.3 g was also observed to have a common behaviour with close trend lines similar to the case of S_S.

For the determination of soil period, the following equation can be used [28]:

$$T = \frac{4H}{V_s}, \quad (1)$$

where H is the depth of soil layer and V_s is the shear wave velocity. According to the equations, if the period is taken as 0.2 s similar to the S_S value and H is taken as 30 m, V_s equals to 600 m/s. If this calculation is performed for $T = 1.0$ s similar to S_1, V_s becomes to 120 m/s. Hence, S_S may be seen as related to a V_{s30} value of 600 m/s and S_1 is related to a V_{s30} value of 120 m/s. When Figure 4(a) is examined, it may be observed that the data points increase and peak around 600 m/s gets smaller afterwards. Figure 4(c) shows a decreasing trend from 120 m/s which is a very small value for the graph. The midvalue of 600 m/s for S_S may be the reason of the more complicated behaviour seen in Figure 4(b) and edge value for S_1 may have led to a more uniform pattern in Figure 4(d).

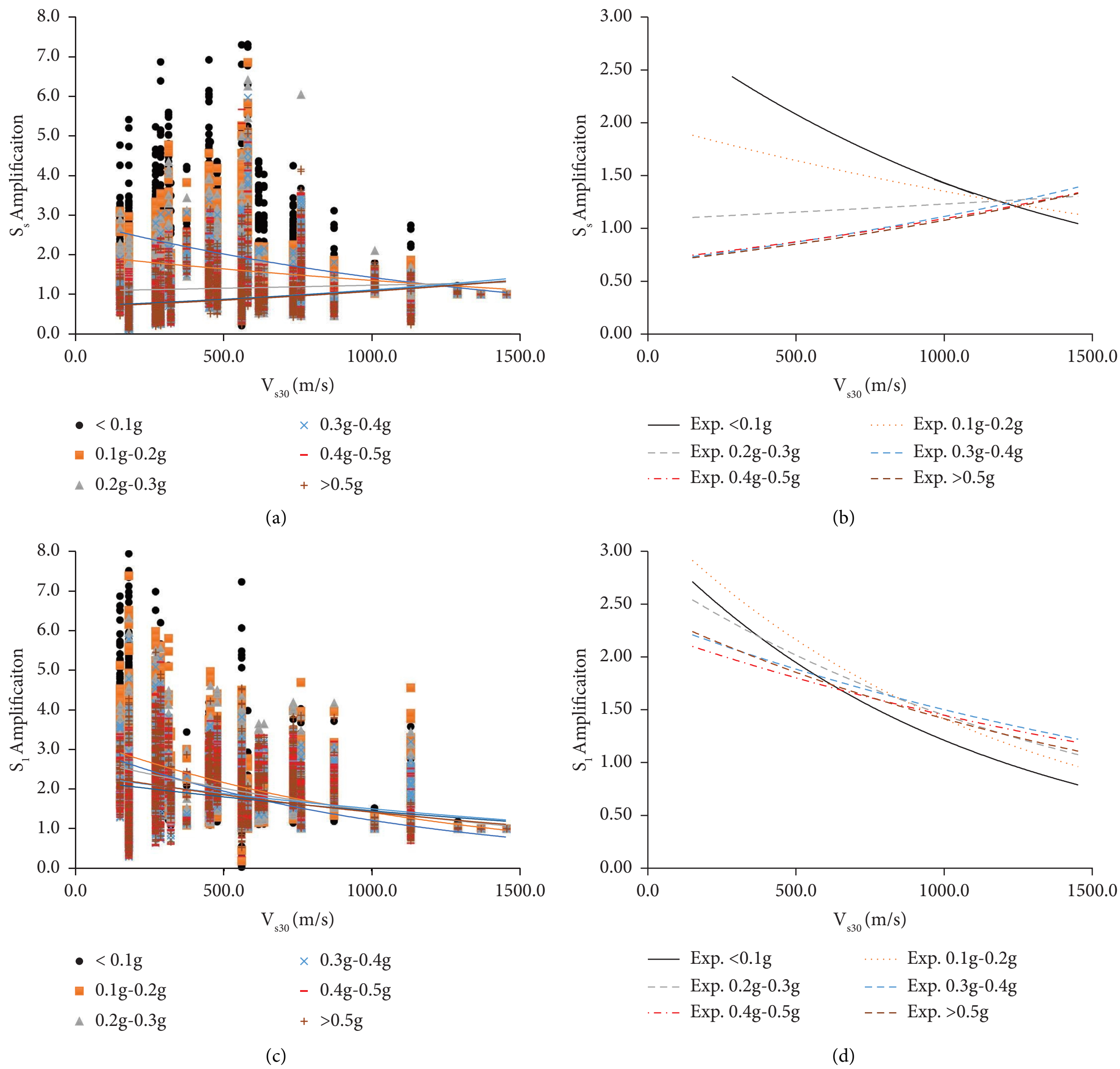

Figure 4: The relationships between V_{s30} and S_S and S_1 amplification. (a) Amplification of S_S with respect to V_{s30}. (b) Amplification of S_S trend lines for different PGA groups. (c) Amplification of S_1 with respect to V_{s30}. (d) Amplification of S_1 trend lines for different PGA groups.

Relations given in Figure 4 are also investigated using soil period and two different ground motion frequency content parameters. Considering soil period showed almost the same picture in backwards as it is inversely proportional to the V_{s30}. Spectral acceleration amplification with respect to ground motion frequency content parameters (e.g., T_{M1} and T_{M2} [49]) seems to have no apparent association.

4.3. Observations on Site Coefficients. The inclusion of local soil conditions is made through site coefficients given in codes as tables for different intensity ground motions. In recent Turkish seismic code [6], both site class definitions and site coefficients are very similar with the 2018 International Building Code [50]. The evaluation method explained here is based on these and resembling codes.

A study was conducted in order to determine the values of the site coefficient table in the seismic codes within the scope of the established acceleration record set. For this aim, first of all, a ground set with a V_{s30} value of 760 m/s, which is taken as the reference ground in the code, is defined. There are 14 records in this set with a V_{s30} value of 745.11 m/s and a maximum difference of 3.5% from 760 m/s. Site coefficients are calculated by dividing the average spectral acceleration values of the acceleration records in each soil group by the average spectral acceleration values of the reference soil set.

Table 2: Number of accounted acceleration records for the short period (S_S) region.

Local site classes	Spectral acceleration groups						
	0.1*	0.25	0.50	0.75	1.00	1.25	1.50
Reference	70	378	182	266	126	42	42
ZB	90	486	234	342	162	54	54
ZC	225	1215	585	855	405	135	135
ZD	90	486	234	342	162	54	54
ZE	45	243	117	171	81	27	27
ZF	45	243	117	171	81	27	27

*Group not included in the codes.

Table 3: Number of accounted acceleration records for the 1.0 s period (S_1) region.

Local site classes	Spectral acceleration groups							
	0.05*	0.10	0.20	0.30	0.40	0.50	0.60	0.70*
Reference	98	196	70	42	112	182	112	56
ZB	126	252	90	54	144	234	144	72
ZC	315	630	225	135	360	585	360	180
ZD	126	252	90	54	144	234	144	72
ZE	63	126	45	27	72	117	72	36
ZF	63	126	45	27	72	117	72	36

*Group not included in the codes.

In this calculation, although it is not taken into account in the codes due to their more specific scope, spectral acceleration rates of $S_S = 0.1$ for the short period and $S_1 = 0.05$ and 0.7 for the 1.0 second period were also examined. The number of acceleration records in each group is given in Tables 2 and 3. Since ZA group V_{s30} is a rarely encountered solid hard rock soil with a value greater than 1500 m/s and the number of relevant data within the scope of the project is limited, it is not included in the analysis.

When Tables 2 and 3 are examined, it is seen that there are different numbers of acceleration records for each group. This is because these values could not be determined at the beginning of the study. Each acceleration record is in a certain group according to the spectral acceleration value obtained after passing through different site definitions. Since these values cannot be estimated at the beginning of the study, a uniform distribution among the groups cannot be expected. However, it may be thought that there are enough earthquake records to have an idea in every group.

Site coefficients obtained within the scope of the study are listed in Tables 4 and 5. The order of values given in the tables are related code value, average value, and value with 84% of probability of not exceedance. Values with a safety of 84% not exceedance are determined using just average values which may not be appropriate for codes that require a certain level of safety and based on an assumption of log-normal distribution [51]. As it is a common value in literature, 84% is used as a safety level [52]. If an explicit value is not given in the codes, it is denoted as "—." For certain values marked as * in Table 4, explicit values are not given in 2018 International Building Code [50] but given in 2018 Turkish Building Seismic Code [6]. The two codes only differ at those points as far as this study concerns.

ZF site class is a special class which requires site-specific evaluation per codes. Site conditions which do not fit common classification are considered in this class and may include broad and divergent conditions. Therefore, the coefficients given in this study may be taken as exemplary and evaluated with additional care.

It is realised that there are differences between the values determined in scope of the study and code given ones. When the short period site coefficients (S_S) values are examined, it is seen that all values obtained in the study for the ZB group are greater than 0.90 which is given in the code. Although the average value is 0.91 for the $S_S \leq 0.25$ group, which is quite close to the regulation, it is around 1.0 for $S_S = 0.50$ and close to 1.10 for all other average values. The code values are approximately 10–20% lower than the average ones obtained in the study. Moreover, the values with assumed 84% safety level are in the range of 1.50–1.70 which is significantly higher than code given ones.

In the ZC group, average values compatible with the code are obtained for the $S_S \leq 0.25$ column. Average values below the regulation values are found after the $S_S = 0.50$ column. However, the values with 84% safety tell a different picture with values roughly around 1.60. For ZC to ZE, many codes' values, given in Table 4, fall into this category, which are significantly higher than average but lower than the 84% safety values. Only three values, $S_S = 0.25$ for ZD, ZE, and $S_S = 0.50$ for ZE, differ which indicate that code values are higher than others. To sum up, all values for ZB indicate the given code values are low, and for mentioned three cases, code values are high. For other site coefficients, the average and 84% safety level indicates different directions.

If ZF is examined by the values given in Table 4, the requirement of site-specific investigation is validated. Excluding ZF in Table 4, around half of the average values is under 1.0 which is an indicator of deamplification. None of the values of ZF is below 1.0 even for high intensity ground motions which is mainly the case for ZC-ZE site classes.

For site coefficients of S_1 region listed in Table 5, all ZB code values are between average and 84% safety level. After $S_1 = 0.1$ ZC, all code values for ZC-ZE are higher than the others indicating overly conservative figures. For ZF, the case is very similar to S_S implying great amplification when compared to other site classes.

Table 4 and especially Table 5 show that the codes generally act on the assumption that ground motions are more amplified by soils with lesser stiffness. In order to understand the amplification process, the events that occur during the transmission of the earthquake wave from the bedrock to the top of the soil profile may be examined. In general, the density and V_s of deep soil layers are higher than those on the surface due to higher overburden pressure. For this reason, an increase in amplitude can be expected due to the decreasing intensity and V_s value of an earthquake wave propagating upwards from the bedrock [28]. It is expected that the acceleration values will increase meaning amplification. However, the large acceleration values cause larger shear stresses on the soil layers. This situation will lead to increased damping ratios. In other words, soft soil layers may not be able to transmit the waves passing through them

Table 4: Site coefficients for the short period (S_S) region.

Local site classes	Site coefficient S_S for code, average, and for 84% safety						
	0.1**	0.25	0.50	0.75	1.00	1.25	1.50
ZB	—/0.85/1.41	0.90/0.91/1.50	0.90/0.99/1.63	0.90/1.09/1.70	0.90/1.09/1.68	0.90/1.09/1.61	0.90/1.09/1.61
ZC	—/1.38/1.64	1.30/1.30/1.66	1.30/1.10/1.63	1.20/0.92/1.67	1.20/0.92/1.65	1.20/0.91/1.58	1.20/0.90/1.57
ZD	—/1.23/1.45	1.60/1.09/1.50	1.40/0.82/1.52	1.20/0.57/1.56	1.10/0.56/1.55	1.00/0.63/1.49	1.00/0.59/1.50
ZE	—/1.07/1.50	2.40/0.83/1.48	1.70/0.55/1.50	1.30/0.33/1.54	1.10*/0.33/1.53	0.90*/0.42/1.50	0.80*/0.36/1.48
ZF	—/1.71/1.75	—/1.62/1.65	—/1.33/1.68	—/1.19/1.71	—/1.20/1.68	—/1.13/1.54	—/1.12/1.54

*Values not included in 2018 IBC [50] but given in 2018 TBC [6]. **Group not included in the codes.

Table 5: Site coefficients for the midperiod (S_1) region.

Local site classes	Site coefficient S_1 for code, average, and for 84% safety							
	0.05**	0.10	0.20	0.30	0.40	0.50	0.60	0.70**
ZB	—/0.81/1.40	0.80/0.77/1.45	0.80/0.78/1.32	0.80/0.76/1.42	0.80/0.73/1.31	0.80/0.73/1.29	0.80/0.72/1.28	—/0.69/1.27
ZC	—/1.08/1.48	1.50/1.11/1.59	1.50/1.12/1.45	1.50/1.05/1.46	1.50/1.08/1.33	1.50/1.08/1.32	1.40/1.10/1.31	—/1.10/1.31
ZD	—/1.51/1.54	2.40/1.54/1.65	2.20/1.50/1.55	2.00/1.60/1.63	1.90/1.39/1.46	1.80/1.19/1.41	1.70/1.16/1.46	—/1.10/1.52
ZE	—/1.98/1.99	4.20/1.42/1.66	3.30/1.24/1.67	2.80/1.19/1.72	2.40/0.90/1.53	2.20/0.74/1.44	2.00/0.72/1.40	—/0.62/1.38
ZF	—/2.26/2.32	—/1.55/1.69	—/1.49/1.55	—/1.21/1.47	—/1.24/1.33	—/1.19/1.32	—/1.14/1.31	—/1.12/1.32

**Group not included in the codes.

with the same intensity due to heightened damping. In this case, these layers can act similar to a damper, leading to the limitation of acceleration values (deamplification). In other words, weak soils can impact the passing ground motion in two different ways. While wave amplitudes are expected to increase due to low density and V_s value during wave propagation, stress and acceleration values may be limited due to increased damping.

Considering lower spectral acceleration values in weak soils seems contrary to common engineering logic, it is considered appropriate by the codes to give larger spectral acceleration values for weak soils, taking into account the first case. However, the observations that weak soils reduce the building damage by limiting the acceleration values are also included in the literature, although it contradicts the general opinion.

Trifunac [53] stated that in March 10, 1933, Long Beach, California earthquake, areas with large ground deformation and different ground movements (determined by breaks in water and gas pipe distribution systems) and areas with heavy building damage showed significant decomposition. The same situation was observed after the 1994 Northridge, California earthquake [54]. Based on these observations, it was concluded that the "simplistic and common" interpretations of building damage due to soft or bad ground conditions in areas close to the earthquake source are wrong, and in fact, it has been claimed that a significant reduction in potential building damage can be expected in areas where moderate to large ground deformations occur [53]. In another study, the damage distributions of the San Fernando 1971 and Northridge 1994 earthquakes were examined, and it was reported that the building damage was less in cases where the soil behaviour went out of the linear region [55]. Supporting results are observed by the similar researches in the literature [13, 18, 56].

4.4. The Variation of Site Coefficient Values. In addition to the level of amplification reflected by site coefficients, the variability of this value based on the soil and ground motion properties is also important. Methods resulting in output values changing in a small range are more representative of the reflected physical phenomenon. In this sense, the standard deviation of the figures given in Tables 4 and 5 are also investigated and illustrated in Figure 5.

When Figure 5 is examined, the approach of "S_S coefficient being related to a V_s value of 600 m/s and S_1 coefficient being related to a V_s value of 120 m/s" explained in Section 4.2 is also useful. The site classes with the highest deviations are the ones closer to the V_s value of 600 m/s, such as ZB and ZC. They have a variation close to ZF which may include site conditions with a wide range of properties. The high variation of the reference site group consisting of close V_s values shows the importance of the scatter coming from acceleration record features on the site coefficient.

For S_1 variation given in Figure 5(b), the site classes close to 120 m/s identified as ZE and ZD come forward. Both figures show that when the period of site class and site coefficient comes closer, the variation increases. This may be attributable to the higher probability of resonance such as behaviour between waves having a period close to the related site coefficient in the ground motion and local site.

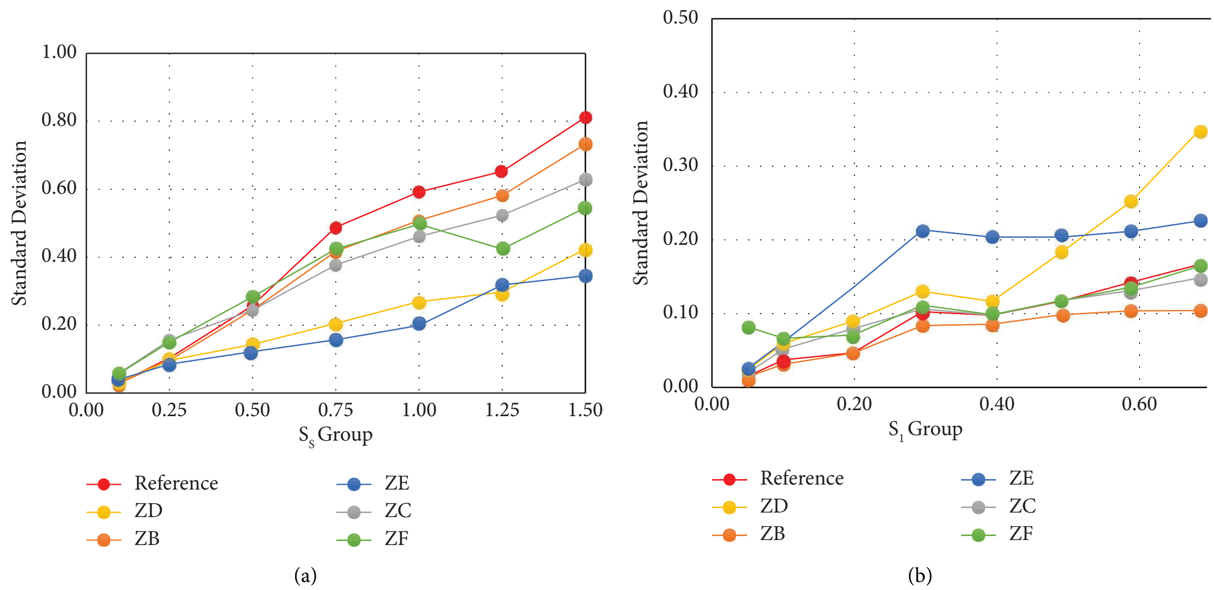

Figure 5: The standard deviation values of S_S for different intensity groups. (a) The standard deviation values of S_S. (b) The standard deviation values of S_1.

5. Summary and Conclusions

A study aiming to investigate site amplification is conducted. A set of 84 ground motion records in a base rock form and targeted to have different frequency contents is formed. The surface forms of these records altered by 100 different soil conditions are determined. By using this set of 8400 ground motion records, site amplification phenomenon is examined. The findings in scope of the current article may be summarized as follows:

(i) During their excursion from bedrock to surface, ground motions may be amplified or deamplified. Even amplification is more pronounced with lower intensities; great amplification values may be observed for all intensity levels.

(ii) For short period site coefficients (S_S), up to 0.5 g amplification is very common for more than 75% of cases. After 0.5 g, amplification occurrence ratio significantly drops to around 0.4 making $S_S = 0.5$ g a corner value.

(iii) For midperiod site coefficients (S_1), amplification is almost certain for low intensities and a general behaviour with an occurrence ratio not much lower than 90% for even with high intensities of $S_1 = 0.6$ g.

(iv) After a PGA of 0.3 g, all ground motions have the same behaviour of increasing S_S amplification with increasing V_{s30} (i.e., soil stiffness) with fully coinciding trend lines. For a PGA of less than 0.2 g, soil amplification observed to be decreasing with increasing soil stiffness.

(v) For S_1 parameter, for all PGA groups, amplification decreases with increasing soil stiffness

(vi) Spectral acceleration amplification with respect to solely ground motion frequency content appears to have no evident association

(vii) Numerical figures as average and with a safety level of 84% for the S_S and S_1 site coefficients per ground motions and site conditions in scope of the study are determined and given in related tables.

(viii) When the given code and values obtained in scope of the study for site coefficients are compared, S_S values for ZB for all intensity ranges seems to be unconservative. Figures for $S_S = 0.25$ for ZD, ZE, and $S_S = 0.50$ for ZE appear to be over conservative. For others, given values may be considered arguable based on the assumed safety level.

(ix) For site coefficient S_1, almost all code given values except for ZB may be claimed to be slightly or greatly over conservative

(x) To sum up, current code consideration is focused on increased soil amplification with decreasing soil stiffness despite some contradicting evidence in the literature. This resulted in unconservative values for stiff soils and too conservative values for soft soils.

(xi) ZF site conditions are observed to have distinctive features when compared to other site classes which validate the requirement of site-specific investigation by the codes. Especially average ZF site coefficients (both S_S and S_1) have a tendency to be higher than almost all the others.

(xii) Linking S_S with a V_s value of 600 m/s and S_1 with a V_s value of 120 m/s seems to be useful to understand some amplification behaviour

(xiii) Variation of value of site coefficients may be related to the linked V_s value. For S_S, the variation of ZB and ZC and for S_1, the variation of ZE and ZD seem to be greater when compared to others.

In the scope of the article, many observations are reported. For future studies, subjects such as unconservative values encountered in the codes for stiffer soils, given corner values for PGA for amplification behaviour, heightened scatter of S_S and S_1 for certain site classes, and behaviour of ZF site class may be investigated more deeply.

Data Availability

The data used to support the findings of this study are available from the corresponding author upon request.

Conflicts of Interest

The author declares that there are no conflicts of interest.

Acknowledgments

This study was supported as the project of "Change of Earthquake Ground Motions Depending on Soil Properties" and grant number 215M357 by the Scientific and Technological Research Council of Turkey (TUBITAK).

References

[1] H. B. Ozmen, "A view on how to mitigate earthquake damages in Turkey from a civil engineering perspective," *Research on Engineering Structures and Materials (RESM)*, vol. 7, pp. 1–11, 2021.

[2] R. D. Borcherdt, "Effects of local geology on ground motion near san francisco rbay," *Bulletin of the Seismological Society of America*, vol. 60, pp. 29–61, 1970.

[3] H. B. Seed, C. Ugas, and J. Lysmer, "Site-dependent spectra for earthquake-resistant design," *Bulletin of the Seismological Society of America*, vol. 66, no. 1, pp. 221–243, 1976.

[4] Bssc Building Seismic Safety Council, *NEHRP Recommended Seismic Provisions for New Buildings and Other Structures: Part 1, Provisions*, BSSC, Building Seismic Safety Council, Washington DC, USA, 2009.

[5] Cen, *Comité Européen de Normalisation. Eurocode 8, Design of structures for earthquake resistance—part 1: General rules, seismic actions and rules for buildings*, European Standard NF EN, Brussels, Belgium, 2004.

[6] Tbsc, *Turkish Building Seismic Code*, Ministry of Environment and Urban Planning, Ankara, Turkey, 2018.

[7] Nzs, *NZS 1170.5: Structural Design Actions and Commentary, Part 5, Earthquake Actions, Wellington, New Zealand*, Internet archive, San Francisco, CA, USA, 2004.

[8] R. D. Borcherdt, "Estimates of site-dependent response spectra for design (methodology and justification)," *Earthquake Spectra*, vol. 10, no. 4, pp. 617–653, 1994.

[9] R. Dobry, R. D. Borcherdt, C. B. Crouse et al., "New site coefficients and site classification system used in recent building seismic code provisions," *Earthquake Spectra*, vol. 16, no. 1, pp. 41–67, 2000.

[10] Y.-N. Huang, A. S. Whittaker, and N. Luco, "NEHRP site amplification factors and the NGA relationships," *Earthquake Spectra*, vol. 26, no. 2, pp. 583–593, 2010.

[11] M. Power, B. Chiou, N. Abrahamson, Y. Bozorgnia, T. Shantz, and C. Roblee, "An overview of the NGA project," *Earthquake Spectra*, vol. 24, no. 1, pp. 3–21, 2008.

[12] R. D. Borcherdt, "Implications of next generation attenuation ground motion prediction equations for site coefficients used in earthquake resistant design," *Earthquake Engineering & Structural Dynamics*, vol. 43, no. 9, pp. 1343–1360, 2014.

[13] M. A. Sandıkkaya, S. Akkar, and P. Bard, "A nonlinear site amplification model for the next Pan European ground motion prediction equations," *Bulletin of the Seismological Society of America*, vol. 103, no. 1, pp. 19–32, 2013.

[14] E. Seyhan and J. P. Stewart, "Semi-empirical nonlinear site amplification from NGA-West2 data and simulations," *Earthquake Spectra*, vol. 30, no. 3, pp. 1241–1256, 2014.

[15] Y. Bozorgnia, N. A. Abrahamson, L. A. Atik et al., "NGA-West2 Research project," *Earthquake Spectra*, vol. 30, no. 3, pp. 973–987, 2014.

[16] Bssc Building Seismic Safety Council, *NEHRP Recommended Seismic Provisions for New Buildings and Other Structures*, BSSC. Building Seismic Safety Council, Washington, DC, USA, 2015.

[17] Asce American Society of Civil Engineers, *Minimum Design Loads for Buildings and Other Structures*, ASCE, American Society of Civil Engineers, Reston, VA, USA, 2016.

[18] R. P. Dhakal, S. L. Lin, A. K. Loye, and S. J. Evans, "Seismic design spectra for different soil classes," *Bulletin of the New Zealand Society for Earthquake Engineering*, vol. 46, no. 2, pp. 79–87, 2013.

[19] P. Lussou, P. Y. Bard, F. Cotton, and Y. Fukushima, "Seismic design regulation codes: contribution of k-net data to site effect evaluation," *Journal of Earthquake Engineering*, vol. 5, no. 1, pp. 13–33, 2001.

[20] E. Işık, A. Büyüksaraç, Y. L. Ekinci, M. C. Aydın, and E. Harirchian, "The effect of site-specific design spectrum on earthquake-building parameters: a case study from the Marmara region (NW Turkey)," *Applied Sciences*, vol. 10, no. 20, p. 7247, 2020.

[21] H. H. Yavaşoğlu, M. N. Alkan, S. Bilgi, and Ö. Alkan, "Monitoring aseismic creep trends in the İsmetpaşa and Destek segments throughout the North Anatolian Fault (NAF) with a large-scale GPS network," *Geoscientific Instrumentation, Methods and Data Systems*, vol. 9, no. 1, pp. 25–40, 2020.

[22] M. Strukar, T. K. Sipos, M. Jelec, and Hadzima-Nyarko, "Efficient damage assessment for selected earthquake records based on spectral matching," *Earthquakes Struct*, vol. 17, pp. 271–282, 2019.

[23] M. A. Sandıkkaya, S. Akkar, and P.-Y. Bard, "A probabilistic procedure to describe site amplification factors for seismic design codes," *Soil Dynamics and Earthquake Engineering*, vol. 126, Article ID 105068, 2019.

[24] Proshake, "EduPro C.S. Inc, ProShake 2.0," 2018.

[25] H. B. Ozmen, H. Yilmaz, and H. Yildiz, "An acceleration record set for different frequency content, amplitude and site classes," *Research on Engineering Structures and Materials*, vol. 5, pp. 321–333, 2019.

[26] T. Beyaz, *Zemin etkisinden arındırılmış deprem kayıtlarına göre türkiye için yeni bir deprem enerjisi azalım bağıntısının geliştirilmesi*, PhD Thesis, Ankara University, Graduate School of Scence, Ankara, Türkiye, 2004.

[27] E. M. Rathje, N. A. Abrahamson, and J. D. Bray, "Simplified frequency content estimates of earthquake ground motions," *Journal of Geotechnical and Geoenvironmental Engineering*, vol. 124, pp. 150–159, 1998.

[28] S. L. Kramer, *Geotechnical Earthquake Engineering*, Springer, Berlin, Germany, 1996.
[29] W. K. Tso, T. J. Zhu, and A. C. Heidebrecht, "Engineering implication of ground motion A/V ratio," *Soil Dynamics and Earthquake Engineering*, vol. 11, no. 3, pp. 133–144, 1992.
[30] L. Xu, J. Hu, and L. Xie, "On characteristics of ground motion parameters for special long-period ground motions," *Earthquake Engineering and Engineering Vibration*, vol. 28, pp. 20–27, 2008.
[31] M. R. Kianoush and A. R. Ghaemmaghami, "The effect of earthquake frequency content on the seismic behavior of concrete rectangular liquid tanks using the finite element method incorporating soil-structure interaction," *Engineering Structures*, vol. 33, no. 7, pp. 2186–2200, 2011.
[32] H. B. Ozmen, "Developing hybrid parameters for measuring damage potential of earthquake records: case for RC building stock," *Bulletin of Earthquake Engineering*, vol. 15, no. 7, pp. 3083–3101, 2017.
[33] J. J. Bommer, J. Douglas, and F. O. Strasser, "Style-of-faulting in ground-motion prediction equations," *Bulletin of Earthquake Engineering*, vol. 1, no. 2, pp. 171–203, 2003.
[34] H. B. Ozmen and M. Inel, "Strength reduction factors for existing mid-rise RC buildings for different performance levels," *Research on Engineering Structures and Materials*, vol. 4, pp. 241–255, 2018.
[35] M. Leti and H. Bilgin, "Damage potential of near and far-fault ground motions on seismic response of RC buildings designed according to old practices," *Research on Engineering. Structure and Material*, vol. 8, no. 2, pp. 337–357, 2022.
[36] E. M. Rathje, F. Faraj, S. Russell, and J. D. Bray, "Empirical relationships for frequency content parameters of earthquake ground motions," *Earthquake Spectra*, vol. 20, no. 1, pp. 119–144, 2004.
[37] F. Naeim, A. Alimoradi, and S. Pezeshk, "Selection and scaling of ground motion time histories for structural design using genetic algorithms," *Earthquake Spectra*, vol. 20, no. 2, pp. 413–426, 2004.
[38] Y. M. Fahjan, "Selection and scaling of real earthquake accelerograms to fit the Turkish design spectra," *Teknik Dergi/ Technical Journal of Turkish Chamber of Civil Engineering*, vol. 19, pp. 4423–4444, 2008.
[39] T. Ucar and O. Merter, "Effect of design spectral shape on inelastic response of RC frames subjected to spectrum matched ground motions," *Structural Engineering & Mechanics*, vol. 63, pp. 293–306, 2019.
[40] S. Vatansever, *Gerçek Deprem Kayıtlarının Ölçekleme Yöntemlerinin Karşılaştırılması*, Gebze Yüksek Teknoloji Enstitüsü, Darıca, Türkiye, 2011.
[41] E. H. Vanmarcke, *State-of-the-Art for Assessing Earthquake Hazards in the United States: Representation of Earthquake Ground Motions – Scaled Accelerograms and Equivalent Response Spectra*, Vicksburg, Mississippi, MS, USA, 1979.
[42] E. L. Krinitzsky and F. K. Chang, *State-of The-Art for Assessing Earthquake Hazards in the United States: Specifying Peak Motions for Design Earthquakes*, US Army Engineer Waterways Experiment Station, Mississippi, MS, USA, 1977.
[43] G. G. Amiri and F. M. Dana, "Introduction of the most suitable parameter for selection of critical earthquake," *Computers & Structures*, vol. 83, no. 8-9, pp. 613–626, 2005.
[44] H. B. Ozmen and M. Inel, "Damage potential of earthquake records for RC building stock," *Earthquakes and Structures*, vol. 10, no. 6, pp. 1315–1330, 2016.
[45] Ö. Avşar and G. Özdemir, "Response of seismic-isolated bridges in relation to intensity measures of ordinary and pulselike ground motions," *Journal of Bridge Engineering*, vol. 18, no. 3, pp. 250–260, 2013.
[46] Ö. Avşar, A. Yakut, and A. Caner, "Analytical fragility curves for ordinary highway bridges in Turkey," *Earthquake Spectra*, vol. 27, no. 4, pp. 971–996, 2011.
[47] H. B. Ozmen, M. Inel, E. Akyol, B. T. Cayci, and H. Un, "Evaluations on the relation of RC building damages with structural parameters after May 19, 2011 Simav (Turkey) earthquake," *Natural Hazards*, vol. 71, no. 1, pp. 63–84, 2014.
[48] M. Walling, W. Silva, and N. Abrahamson, "Nonlinear site amplification factors for constraining the NGA models," *Earthquake Spectra*, vol. 24, no. 1, pp. 243–255, 2008.
[49] Tubitak, *Change of Earthquake Ground Motions Depending on Soil Properties, 215M357*, Tubitak, Usak, Turkey, 2019.
[50] Icc, *International Building Code -2018*, ICC, Washington, DC, USA, 2018.
[51] J.-P. Wang, C.-H. Chan, and Y.-M. Wu, "The distribution of annual maximum earthquake magnitude around Taiwan and its application in the estimation of catastrophic earthquake recurrence probability," *Natural Hazards*, vol. 59, no. 1, pp. 553–570, 2011.
[52] K. Pitilakis, E. Riga, and A. Anastasiadis, "New code site classification, amplification factors and normalized response spectra based on a worldwide ground-motion database," *Bulletin of Earthquake Engineering*, vol. 11, no. 4, pp. 925–966, 2013.
[53] M. D. Trifunac, "Nonlinear soil response as a natural passive isolation mechanism. Paper II. The 1933, Long Beach, California earthquake," *Soil Dynamics and Earthquake Engineering*, vol. 23, no. 7, pp. 549–562, 2003.
[54] M. D. Trifunac and M. I. Todorovska, "Nonlinear soil response as a natural passive isolation mechanism—the 1994 Northridge, California, earthquake," *Soil Dynamics and Earthquake Engineering*, vol. 17, no. 1, pp. 41–51, 1998.
[55] M. D. Trifunac and M. I. Todorovska, "1971 San Fernando and 1994 Northridge, California, earthquakes: did the zones with severely damaged buildings reoccur?" *Soil Dynamics and Earthquake Engineering*, vol. 24, no. 3, pp. 225–239, 2004.
[56] R. D. Hoult, E. Lumantarna, and H. M. Goldsworthy, "Soil amplification in low-to-moderate seismic regions," *Bulletin of Earthquake Engineering*, vol. 15, no. 5, pp. 1945–1963, 2017.